PHYSICAL REVIEW D **91,** 025021 (2015)

Topological order and the vacuum of Yang-Mills theories

G. Burgio and H. Reinhardt

Institut für Theoretische Physik, Auf der Morgenstelle 14, 72076 Tübingen, Germany

(Received 4 December 2014; published 27 January 2015)

We study, for $SU(2)$ Yang-Mills theories discretized on a lattice, a nonlocal topological order parameter, the center flux z. We show that i) well-defined topological sectors classified by $\pi_1(SO(3)) = \mathbb{Z}_2$ can only exist in the ordered phase of z; ii) depending on the dimension $2 \leq d \leq 4$ and action chosen, the center flux exhibits a critical behavior sharing striking features with the Kosterlitz-Thouless type of transitions, although belonging to a novel universality class; and iii) such critical behavior does not depend on the temperature T. Yang-Mills theories can thus exist in two different continuum phases, characterized by an either topologically ordered or disordered vacuum; this reminds us of a quantum phase transition, albeit controlled by the choice of symmetries and not by a physical parameter.

DOI: 10.1103/PhysRevD.91.025021 PACS numbers: 11.15.Ha, 12.38.Aw

I. INTRODUCTION

Of all ideas applied to the confinement problem in non-Abelian Yang-Mills theories [1,2], the most popular still involve topological degrees of freedom of some sort [3–11]. Among these, center vortices [12–14] have enjoyed broad attention, in particular, in the lattice literature. Although most of the effort was put in dealing with gauge fixed schemes,[1] some investigations actually attempted to tackle the problem in a gauge invariant way [17–23] and are therefore directly related to 't Hooft's original idea.

$SU(N)$ non-Abelian gauge field theories transform under the group's adjoint representation, $SU(N)/\mathbb{Z}_N$. Such a group is not simply connected, with a nontrivial first homotopy class:

$$\pi_1\left(\frac{SU(N)}{\mathbb{Z}_N}\right) = \mathbb{Z}_N, \tag{1}$$

the center of $SU(N)$. Following Ref. [13], let us consider the Euclidean Yang-Mills theory on a d-dimensional torus,[2] i.e., with all directions compactified, and choose one of the d Euclidean directions as time. If large gauge transformations classified by Eq. (1) induce a superselection rule, we can decompose the physical Hilbert space $\mathcal{H}$ of gauge invariant states [25] in subspaces $\mathcal{H}_{\vec{k},\vec{m}}$ labeled by topological indices, the $\mathbb{Z}_N$ electric and magnetic fluxes (vortices) $\vec{k} = (k_1, \ldots, k_{n_t})$ and $\vec{m} = (m_1 \ldots, m_{n_s})$ [13]:

$$\mathcal{H} = \bigoplus_{k_i, m_j = 0}^{N-1} \mathcal{H}_{\vec{k},\vec{m}}. \tag{2}$$

Here, $n_t = d - 1$ counts the space-time, $n_s = \frac{(d-1)(d-2)}{2}$ counts the space-space planes, and $k_i, m_i \in \mathbb{Z}_N$. As 't Hooft pointed out, a sufficient condition for confinement is realized if the low-temperature phase of pure Yang-Mills theories corresponds to a superposition of all (electric) sectors, while above the deconfinement transition, such $\mathbb{Z}_N$ symmetry must get broken to the trivial topological sector [12,13].[3]

One can check such a scenario by calculating, e.g., in lattice simulations, how the free energy for $\mathbb{Z}_N$ flux creation

$$F(\vec{k}) = \Delta\mathcal{U}_{\vec{k}} - T\Delta\mathcal{S}_{\vec{k}} = -\log\frac{Z(\vec{k})}{Z(\vec{0})} \tag{3}$$

changes with the temperature T across the deconfinement transition. Here, $\Delta\mathcal{U}_{\vec{k}}$ is the energy (action) cost to generate the $\vec{k}$th (electric) vortex from the vacuum, $\Delta\mathcal{S}_{\vec{k}}$ is the corresponding entropy change, and $Z(\vec{k})$ is the partition function restricted to the topological sector labeled by $\vec{k}$.[4] For the one-vortex sector, F is nothing but the free energy of a maximal 't Hooft loop,[5] giving a confinement criterion dual to Wilson's: in the thermodynamic limit, F should vanish in the confined phase, while it should diverge as $\tilde{\sigma}(T)L^2$ above the deconfinement temperature T_c, where $\tilde{\sigma}(T)$ is the dual string tension [2,13,17–21,27]. In other words, a perimeter law for the Wilson loop implies an area law for the 't Hooft loop and vice versa [12,13].

Of course, when considering the theory at $T = 0$, the distinction between electric and magnetic fluxes is artificial. In this case *all* the $N^{\frac{d(d-1)}{2}}$ topological sectors must be

[1]See, e.g., Refs. [15,16] for early results and Ref. [2], Chaps. 6 and 7, for a comprehensive review. The goal here is to isolate some relevant degrees of freedom, usually called P vortices, assumed to be related to 't Hooft's topological excitations; we will comment on this in Sec. IV.

[2]See, e.g., Ref. [24] for an extensive introduction to the subject.

[3]Magnetic sectors, on the other hand, can remain unbroken and be responsible for screening effects.

[4]In the deconfined phase, all electric sectors must be suppressed relatively to the trivial one, while in the confined phase, all $\vec{k}$ and $\vec{m}$ should be equally probable.

[5]For a representation of the 't Hooft loop in the continuum, see Ref. [26]

taken into account when establishing whether $\mathbb{Z}_N$ symmetry is unbroken, i.e., whether the vacuum $|\Psi_0\rangle$ is indeed a symmetric superposition of states belonging to $\mathcal{H}_{\vec{k},\vec{m}}$[6]:

$$|\Psi_0\rangle = \sum_{\vec{k},\vec{m}} |\Psi_0^{\vec{k},\vec{m}}\rangle. \tag{4}$$

In the following, we will use either definition, depending on whether we are considering the $T = 0$ or the $T > 0$ case.

The above ideas generalize naturally to the lattice discretization of Yang-Mills theories; the specific action used plays, however, a key role in their actual implementation. If one wishes to preserve the symmetries of the continuum theory, the natural choice should fall on a discretization transforming under the "correct" group $SU(N)/\mathbb{Z}_N$. One possibility among many (see, e.g., Ref. [28]) is given by the adjoint Wilson action with periodic boundary conditions [27],

$$S_A = \beta_A \sum_P \left(1 - \frac{1}{N^2-1} \mathrm{Tr}_A U_P\right), \tag{5}$$

where U_P is the standard plaquette. For $N = 2$, it was indeed shown in Refs. [21,22,29] that for simulations based on Eq. (5) the following are true:

(i) $\mathbb{Z}_2$ topological sectors are well defined in the continuum limit, both below and above T_c; i.e., the decomposition in Eq. (2) holds.
(ii) The partition function $Z_A = \int \exp(-S_A)$ dynamically includes all sectors.
(iii) In the deconfined phase, all nontrivial sectors are suppressed, while as $T \to 0$, all sectors are equivalent; i.e., the vacuum can be described by Eq. (4).

The main difficulty of such a setup lies of course in the implementation of an algorithm capable of tunneling ergodically among all vortex topologies. Simulations are therefore quite demanding: reaching enough statistics to check whether the symmetry among sectors postulated in Eq. (2) remains unbroken from $T = 0$ all the way up to T_c is difficult; the evidence given in Refs. [21,22] seems to point to a more complicated picture.

Alternatively, universality [30] should allow the use of the fundamental Wilson action,

$$S_F = \beta_F \sum_P \left(1 - \frac{1}{N} \Re[\mathrm{Tr}_F U_P]\right), \tag{6}$$

which is the quenched (mass $\to \infty$) limit of the physical action coupling Yang-Mills theories to fundamental fermions, e.g., full QCD. In this case, however, some care must be taken in defining a $SU(N)/\mathbb{Z}_N$ invariant theory. Indeed, in the presence of fundamental fermions, the topological classification of Eq. (1) breaks down.[7] The extension to full QCD has been indeed one of the main obstacles in establishing the 't Hooft vortex picture as a viable model for confinement. We will comment on this in Sec. IV; for the moment, let us note that one can still introduce vortex topological sectors "statically" by simply imposing twisted boundary conditions [19,20,27].[8] We should then be able to reconstruct the "full" partition function Z_F by taking the weighted sum of all partition functions $Z_F(\vec{k},\vec{m}) = \int \exp(-S_F(\vec{k},\vec{m}))$ with boundary conditions corresponding to the sector labeled by $\vec{k}$ and $\vec{m}$ [19,20]. Since each $Z_F(\vec{k},\vec{m})$ must be determined via independent simulations, their relative weights can only be calculated through indirect means.[9] Still, such simulations are computationally more efficient than in the Z_A case and have therefore been the method of choice in most investigations of Eq. (3) [17–20,23].

Investigations using Eq. (6) rely on the assumption that fixing the boundary conditions is enough to ensure that the Hilbert-space decomposition defined in Eq. (2) works. However, it is well known that upon discretization of Yang-Mills theories $\mathbb{Z}_N$ magnetic monopoles are generated at strong coupling [28,35–39], causing bulk phenomena in the $\beta_F - \beta_A$ phase diagram. Now, since the $\mathbb{Z}_N$ fluxes defining our topological sectors live on the coset of a two dimensional plane, they have a simple geometrical interpretation: they are described in $d = 4$ by a *closed* world sheet, i.e., they are stringlike objects, and in $d = 3$ by a closed worldline, i.e., particlelike. On the other hand, topological lattice artifacts as the above-mentioned $\mathbb{Z}_N$ monopoles are themselves sources of $\mathbb{Z}_N$ flux: in $d = 4$, they will be particlelike objects, their closed worldlines bounding *open* $\mathbb{Z}_N$ flux world sheets, while in $d = 3$, they will be instantonlike objects and will be end points of open $\mathbb{Z}_N$ flux lines [27,35–37,39]. $\mathbb{Z}_N$ monopoles are therefore in one-to-one correspondence with open center vortices; in other words, universality between the fundamental and adjoint actions can only be invoked when just closed, i.e., truly topological, $\mathbb{Z}_N$ vortices winding around the compactified directions can form. Notice how in $d = 2$, where no $\mathbb{Z}_N$ monopoles can exist, $\mathbb{Z}_N$ fluxes are instanton-type objects. The distinction between open and closed vortices is in this case blurred, but in a nonergodic setup it can eventually be made through the flux allowed by the boundary conditions chosen.

[6] Actually, in virtue of cubic symmetry, one can regard the subspaces $\mathcal{H}_{\vec{k},\vec{m}}$ with indices equal up to a permutation as equivalent and recombine them in Eq. (4) into weights given by their combinatorial multiplicity [17–19].

[7] See, e.g., Ref. [31] for a recent discussion.

[8] Such topological boundary conditions, relevant, e.g., in investigations of large N reduction [24,32,33], allow adjoint fermions but no fundamental ones. Flavor twisted boundary conditions, on the other hand, are well established in full QCD [34].

[9] See, e.g., Ref. [23], Chap. 3, for a detailed review of the methods involved.

The above discussion has a straightforward consequence. If one could "measure" whether open $\mathbb{Z}_N$ vortices are absent in a given discretization, i.e., whether only topological vortices can be generated from the vacuum, there would be no need to monitor $\mathbb{Z}_N$ monopoles to establish universality between S_A and S_F in the first place, since these must be absent anyway. This would have two advantages. First, such a criterion could be generalized to $d = 2$. Second, the absence of lattice artifacts, whether for S_F, for S_A, or for both, would get "promoted" to a necessary condition for the superselection rule of Eq. (2), and hence for the conjectured vacuum symmetry of Eq. (4), to be realized. Indeed, consider states belonging to distinct topological sectors labeled by the indices k, $k' \in \mathbb{Z}_N$. The presence of open vortices immediately blurs the distinction among them; does the state pictured at the top of Fig. 1 belong to the kth sector, resulting from the superposition of k closed vortices with $\mathrm{mod}(k'-k)_N$ open ones (middle picture), or does it belong to the k'th sector, coming from the superposition of k' closed vortices with $\mathrm{mod}(k-k')_N$ open ones winding in the other direction (bottom picture)? Clearly, there is no way to distinguish between them and assign the configuration to $Z(k)$ rather than $Z(k')$ in Eq. (3). In other words, a Wilson loop will never know if the vortex piercing it to generate the area law for its expectation value [12,13] is open or closed; a confinement criterion based on the vortex free energy F and hence on the 't Hooft loop can only make sense if open vortices are absent at any temperature.

In this paper, we will investigate a topological order parameter, the center flux z, for the transition between phases characterized by the presence of open or closed $\mathbb{Z}_2$ vortices in $SU(2)$ Yang-Mills theories at $T = 0$, discretized through standard plaquette actions. We will show that, depending on the action, the dimensions, and the volume, the theory can be either in a topologically ordered or disordered phase; such a distinction will persist at finite T. In the disordered phase, open vortices dominate the vacuum, and $\mathbb{Z}_2$ topological sectors are ill defined; the Hilbert space of Yang-Mills theories cannot be classified by a superselection as in Eq. (2). Such a disordered phase is compatible with the presence of fundamental fermions; the ordered phase, on the other hand, should be the correct one when coupling $SU(2)$ with adjoint fermions, a popular candidate for infrared conformal gauge theories.

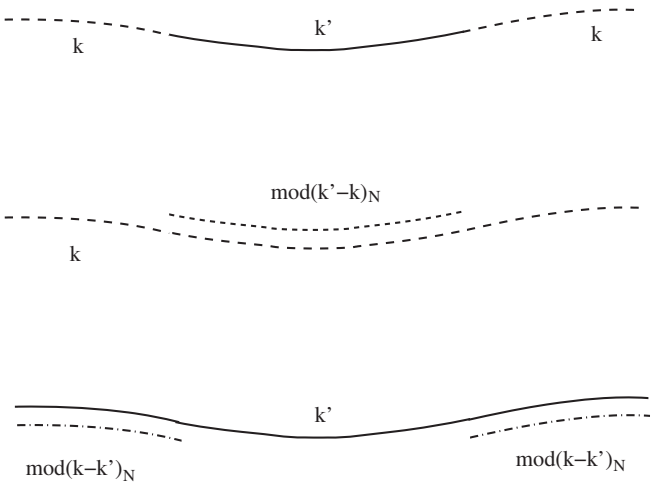

FIG. 1. Illustration of the ambiguity in labeling the $\mathbb{Z}_N$ topological sectors in the presence of open vortices. Should the given configuration (top) be counted to the kth (middle) or to the k'th (bottom) sector?

Besides this (perhaps lengthy) introduction, the rest of the paper is organized as follows. Section II contains details on the lattice setup, observables, and simulation techniques. In Sec. III, the main results will be presented. Section IV contains the conclusions and outlook. Preliminary results of this investigations have been presented in Refs. [40,41].

II. SETUP

A. Action and observables

We will consider the $SU(2)$ mixed fundamental-adjoint Wilson action with periodic boundary conditions in $2 \le d \le 4$ Euclidean dimensions, as given in Eqs. (5) and (6),

$$S = \beta_A \sum_P \left(1 - \frac{1}{3}\mathrm{Tr}_A U_P\right) + \beta_F \sum_P \left(1 - \frac{1}{2}\mathrm{Tr}_F U_P\right)$$
$$\frac{1}{a^{4-d}g^2} = \frac{1}{4}\beta_F + \frac{2}{3}\beta_A, \tag{7}$$

where a is the (dimensionful) lattice spacing and U_P denotes the 1×1 plaquette; all results can be easily generalized to different boundary conditions. For higher groups $SU(N)$, the general picture should not change dramatically [29,42–46]. However, other representations than just the fundamental and adjoint are allowed. Many details might therefore depend on N; direct investigations of at least the $SU(3)$ case would be welcome.

In $d \ge 3$, $\mathbb{Z}_2$ monopoles can be defined for each elementary cube c through the product,

$$\sigma_c = \prod_{P \in \partial c} \mathrm{sign}(\mathrm{Tr}_F U_P), \tag{8}$$

over all plaquettes U_P belonging to its surface ∂c [27–29,38,47]. Notice how rescaling any link by a $\mathbb{Z}_2$ factor will leave σ_c unchanged.

The $\mathbb{Z}_2$ monopole density should vanish in the continuum limit $g^2 \to 0$. This happens, however, in different ways, depending on the dimensions d or the direction along which such a limit is taken in the $\beta_F - \beta_A$ plane, and has been the subject of intense investigations in the pioneering years of lattice gauge theories [38,42–46,48–54]. For the $SU(2) - SO(3)$ case considered here, the resulting phase

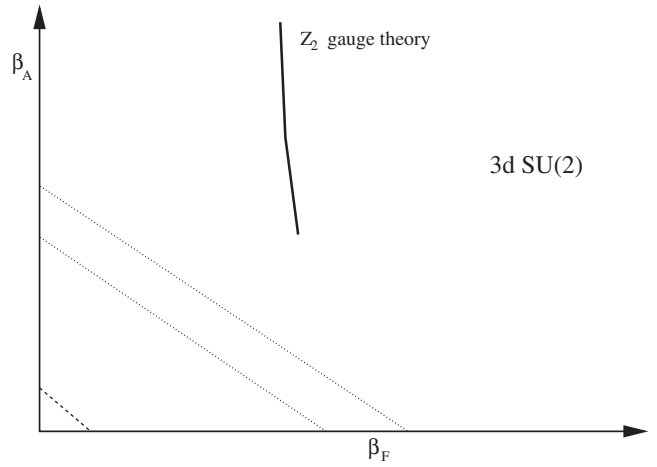

FIG. 2. Phase diagram of the fundamental-adjoint plane for $d = 3$. Continuous lines indicate bulk transitions, dashed lines indicate the roughening transition, and dotted lines indicate the crossover regions associated with $\mathbb{Z}_2$ monopoles. Similar diagrams hold for higher N.

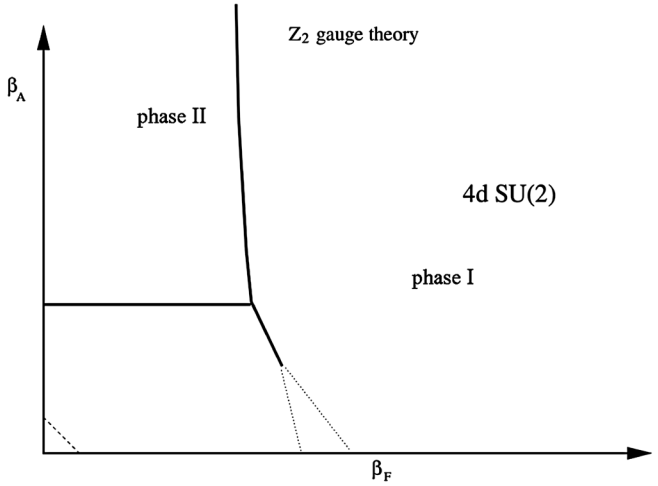

FIG. 3. Phase diagram of the fundamental-adjoint plane for $d = 4$. Continuous lines indicate bulk transitions, dashed lines indicate the roughening transition, and dotted lines indicate the crossover regions associated with $\mathbb{Z}_2$ monopoles. Similar diagrams hold for higher N.

diagrams in $d = 3$ and 4 are sketched in Figs. 2 and 3, and similar ones have been established for $N \geq 3$; see, e.g., Refs. [42–46]. Continuous lines indicate bulk transitions [38,49,50,52], dashed lines indicate the roughening transition [48], and dotted lines indicate the crossover regions associated with $\mathbb{Z}_2$ monopoles [38,52]. The vertical bulk transition line coming down form $\beta_A = \infty$ corresponds to the underlying $\mathbb{Z}_2$ gauge theory: in $d = 3$, it ends at a finite point [52–54], while in $d = 4$, it joins the bulk transition line associated with $\mathbb{Z}_2$ monopoles [38,49,50]. From the endpoint of the latter, a crossover region starts, extending beyond the β_F axis. In $d = 2$, $\mathbb{Z}_2$ monopoles are of course absent. Furthermore, the $\mathbb{Z}_2$ gauge theory has no phase transition; apart from the roughening transition [48], the corresponding phase diagram should therefore be free of any bulk effects, including crossovers.

From Fig. 3, it is obvious that two distinct continuum limits in $d = 4$ exist, depending if $g^2 \to 0$ in Eq. (7) is taken within phase I or II. Phase II at fixed twist has been shown in Refs. [27,29] to be equivalent to a positive plaquette model [14,55,56] with fixed twisted boundary conditions. Although such a model and the fundamental Wilson action seem to describe the same physics, the two phases are always separated by a bulk transition line.[10] What is thus the difference, if any, between them?

A first hint toward an explanation to this (long neglected) puzzle is given by the results of Refs. [21,22,29,47,57–62]: in the continuum limit, the $d = 4$ adjoint theory ($\beta_F \equiv 0$), which lies precisely within phase II, possesses well-defined $\mathbb{Z}_2$ topological sectors, i.e., no open vortices, and the Hilbert-space decomposition defined in Eq. (2) works. On the other hand, one can easily check that in phase I, across all crossovers, the $\mathbb{Z}_2$ monopole density vanishes quite slowly as $g^2 \to 0$; their persistence in the weak coupling phase should reflect itself in the presence of open $\mathbb{Z}_2$ vortices, possibly spoiling Eq. (2). Could the difference between phases I and II lie in whether such a superselection rule is indeed realized for the Hilbert space of Yang-Mills theories? To find out, we can start from the twist operator, which "counts" the $\mathbb{Z}_2$ vortices piercing all parallel planes for a fixed choice of μ-ν [13,27]:

$$z_{\mu\nu} = \frac{1}{L^{d-2}} \sum_{\hat{y} \perp \mu\nu\text{-plane}} \prod_{\hat{x} \in \mu\nu\text{-plane}} \mathrm{sign}(\mathrm{Tr}_F U_{\mu\nu}(\hat{x}, \hat{y})). \quad (9)$$

$U_{\mu\nu}$ and $\hat{x}$, respectively, denote a 1×1 plaquette and point lying in the μ-ν plane, while $\hat{y}$ denotes a point on its coset, which is obviously empty in $d = 2$; only a single plane contributes to the sum in this case. Notice how $z_{\mu\nu}$, like σ_c, is unaffected by any multiplication of links by a center element; i.e., it is insensitive to the spurious $\mathbb{Z}_2$ gauge degrees of freedom.

If topological sectors are well defined, all parallel planes will contribute with the same sign to the sum in Eq. (9). For any fixed μ and ν, $z_{\mu\nu}$ can thus only take the values ± 1, depending on the boundary conditions chosen.[11] For example, for the periodic boundary conditions considered

[10]The authors of Ref. [27] also proved that the first-order line separating the two phases is just a finite volume effect: at high enough volume, phases I and II will be always separated by a second-order line.

[11]Only for $\beta_F = 0$, i.e., along the β_A axis, the $z_{\mu\nu}$ are allowed to tunnel among different topological sectors, provided that an ergodic algorithm capable of overcoming the large barriers among them is used. In this case, the $z_{\mu\nu}$ can take both values ± 1 [21,62].

in this paper, the topological sector must always be trivial: $z_{\mu\nu} \equiv 1 \; \forall \, \mu, \nu$. When, however, topological sectors are ill defined, the contributions to the sum in Eq. (9) can change from plane to plane; in particular, if open $\mathbb{Z}_2$ vortices pierce the planes randomly, all $z_{\mu\nu}$ will average to zero. To make such a statement quantitative and characterize how the transition from the disordered to the ordered regime takes place, we define a (nonlocal) order parameter, the center flux z, such that its expectation value $\langle z \rangle \equiv 1$ if, whatever the boundary conditions, vortex topology takes the correct value expected from the superselection rule, while $\langle z \rangle \equiv 0$ when $\mathbb{Z}_2$ fluxes are maximally randomized. For $d \geq 3$,

$$z = \frac{2}{d(d-1)} \sum_{\mu > \nu = 1}^{d} |z_{\mu\nu}|, \tag{10}$$

while for $d = 2$, since $|z_{12}| \equiv 1$, we will define

$$z = 1 - |z_{12} - \langle z_{12} \rangle|. \tag{11}$$

Notice that the latter definition will only work as long as $\beta_F \neq 0$, i.e., when the $d = 2$ theory cannot tunnel among topological sectors.[12] In the following, we will investigate, either analytically (in $d = 2$) or via Monte Carlo simulations (for $d \geq 3$), the behavior of the center flux and its susceptibility[13]:

$$\chi_z = L^d (z - \langle z \rangle)^2. \tag{12}$$

B. Algorithm

Simulations for $\beta_A = 0$, i.e., along the β_F axis, have been performed using a standard heat-bath algorithm followed by microcanonical steps. Although this cannot be extended to $\beta_A \neq 0$, as long as also $\beta_F \neq 0$, one can use the biased Metropolis + microcanonical algorithm introduced in Refs. [63,64].[14] The lookup tables for the pseudo-heat-bath probability need to be fixed beforehand; sizes between 32×32 and 64×64 were found to be sufficient [63,64]. As long as $\beta_F \gg \beta_A$, the algorithm is for all practical purposes just as efficient as a heat bath, as the amount of accepted proposals stays well above 95%. On the other hand, whenever $\beta_F \ll \beta_A$, the rejected pseudo-heat-bath and microcanonical updates increase considerably. This becomes a real issue when simulating around the peaks of the susceptibility Eq. (12), where autocorrelations for z and χ_z become quite large.[15] One can try to combat such critical slowing down,[16] unavoidable when dealing with any phase transition, by increasing the number of microcanonical steps per biased Metropolis update. Unfortunately, this turns out to be less efficient than for the $\beta_F \gtrsim \beta_A$ case or for the heat-bath algorithm; only with runs of order $\sim 10^8$ sweeps does one eventually reach a good signal-to-noise ratio for χ_z. Since the $d = 3$ case will anyway turn out to be the most interesting from the point of view of the critical behavior, while in $d = 2$ analytic results allow us to otherwise gain control of the problem, we have limited a precise finite size scaling (FSS) [67] analysis to determine the properties of the transition to the $\beta_A = 0$, $d = 3$ case. Still, we have performed simulations for a whole range of parameters and lattice sizes L in $2 \leq d \leq 4$, trying to explore the whole $\beta_F - \beta_A$ plane. We have nevertheless avoided phase II of the $d = 4$ phase diagram in Fig. 3, since it would have called for completely different simulation techniques; see Refs. [21,22,29,47,57–62] for results in this parameter region.

III. RESULTS

A. $d = 2$

The $SU(2)$ theory in $d = 2$ offers the chance to tackle our problem analytically [68,69]. The probability distribution for the mixed action in Eq. (7) reads

$$d\rho(\theta, \beta_F, \beta_A) \propto d\theta \sin^2\theta e^{\beta_F \cos\theta + \frac{4}{3}\beta_A \cos^2\theta} \tag{13}$$

so that the probability for a plaquette to have negative trace is simply given by

$$p(\beta_F, \beta_A) = \frac{\int_{\frac{\pi}{2}}^{\pi} d\theta \sin^2\theta e^{\beta_F \cos\theta + \frac{4}{3}\beta_A \cos^2\theta}}{\int_{0}^{\pi} d\theta \sin^2\theta e^{\beta_F \cos\theta + \frac{4}{3}\beta_A \cos^2\theta}}. \tag{14}$$

The limiting cases $\beta_{F,A} \to 0, \infty$ can be carried out explicitly, giving

$$\begin{aligned} p(\beta_F \equiv 0, \beta_A) &= \frac{1}{2} \\ p(\beta_F \equiv \infty, \beta_A) &= 0 \end{aligned} \tag{15}$$

[12] The definition of the center flux in $d = 2$ might also be adjusted to the pure adjoint theory as long as no ergodic algorithm is available in the ordered phase. The issue is similar to that encountered for, e.g., an Ising model when simulating the low-temperature phase with a cluster algorithm.

[13] Since z is nonlocal, one could argue that the volume factor should be substituted by the number of planes $\frac{d(d-1)}{2} L^{d-2}$. This would, however, just change the critical exponent for χ_z from $L^\gamma \to L^{\gamma - 2}$, which could be reabsorbed in the definition of the hyperscaling relations. Moreover, for each plane up to L^2, vortices can form, summing up again to L^d. To underline the analogies of our results with the Kosterlitz-Thouless literature, we will thus stick to the standard definition. Anyhow, critical behaviors are controlled by a diverging correlation length ξ, which remains unaffected by any rescaling of χ_z.

[14] See, e.g., Ref. [65] for a recent application. A similar algorithm had been proposed in Ref. [66] for $SU(3)$.

[15] Other observables remain, on the other hand, mostly unaffected.

[16] The critical slowing down appears, of course, also in the limit $g^2 \to 0$, i.e., for large β_F and/or β_A.

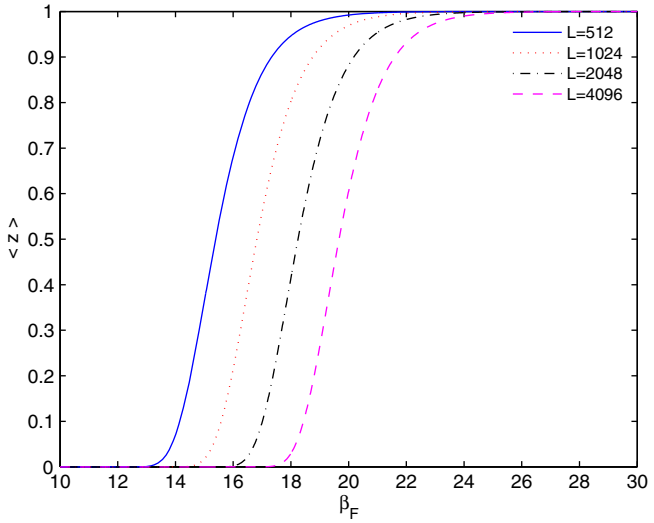

FIG. 4 (color online). Order parameter $\langle z \rangle$ in $d = 2$ along β_F for $L = 512$, 1024, 2048, and 4096.

$$p(\beta_F, \beta_A \equiv 0) = \frac{1}{2}\left[1 - \frac{L_1(\beta_F)}{I_1(\beta_F)}\right]$$
$$p(\beta_F, \beta_A \equiv \infty) = \frac{1}{1 + e^{2\beta_F}}, \tag{16}$$

where L and I denote the modified Struve and Bessel functions, respectively [70].

For fixed volume L^2, the order parameter z and its susceptibility χ_z are given by [71][17]

$$\langle z \rangle = e^{-4L^2 p(\beta_F, \beta_A)}$$
$$\langle \chi_z \rangle = L^2 [e^{-4L^2 p(\beta_F, \beta_A)} - e^{-8L^2 p(\beta_F, \beta_A)}]. \tag{17}$$

The above expressions are plotted, for $\beta_A = 0$, in Figs. 4 and 5; a similar behavior extends to the whole (β_F, β_A) plane, see Fig. 6, where the center flux is plotted for fixed $L = 128$.

We can clearly distinguish a low β_F, "strong" coupling regime, in which $\langle z \rangle = 0$ and the topology is ill defined, from a high β_F, "weak" coupling one, in which $\langle z \rangle = 1$, the correct value it should have if the vacuum satisfies Eq. (4). For higher L, the transition "front" simply moves to the right, i.e., higher β_F; see Fig. 7, in which the curves along which the susceptibility χ_z peaks are plotted for $L = 64$, 256, 1024, and 4096.

As usual in a FSS analysis, we can determine the properties of the transition by defining the pseudocritical couplings $(\beta_F^c(L), \beta_A^c(L))$ at finite L as those for which the correlation length $\xi \simeq L$ [67]. These can be identified through the peaks of the susceptibility χ_z (see Fig. 7); since $p(\beta_F, \beta_A)$ has no stationary points, from Eq. (17), one simply needs to solve

$$p(\beta_F^c, \beta_A^c) = \frac{\log 2}{4L^2}. \tag{18}$$

Substituting the above value into Eq. (17), we get for the scaling of the center flux and its susceptibility with L

$$z(\beta_F^c, \beta_A^c) = \frac{1}{2}$$
$$\chi_z(\beta_F^c, \beta_A^c) = \frac{L^2}{4}. \tag{19}$$

[17]We are indebted to F. Bursa for precious correspondence on the derivation of the above expressions for z and χ_z. Just to be on the safe side, we have also cross-checked all analytic results with Monte Carlo simulations up to $L = 1024$; these become, of course, inefficient as β_A gets large.

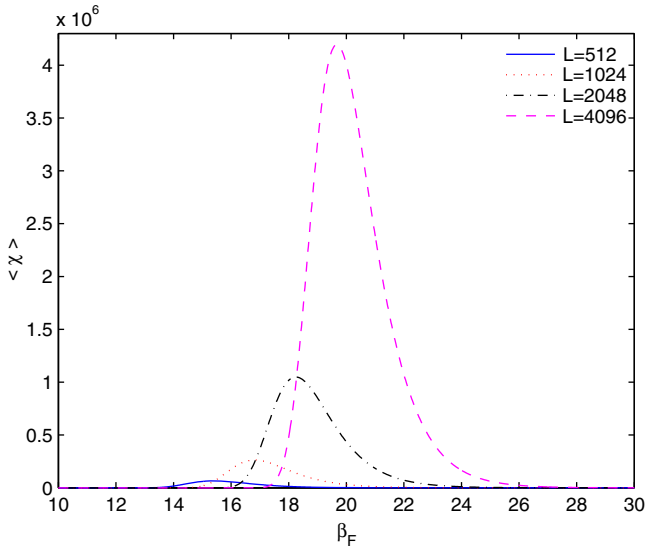

FIG. 5 (color online). Susceptibility χ_z in $d = 2$ along β_F for $L = 512$, 1024, 2048, and 4096.

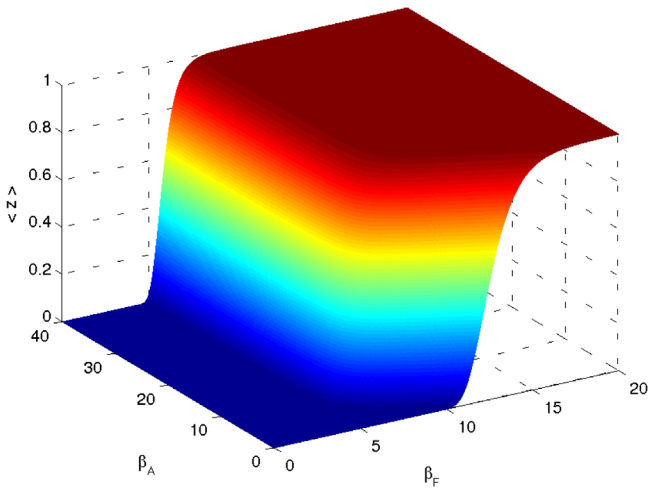

FIG. 6 (color online). Order parameter $\langle z \rangle$ in $d = 2$ for fixed $L = 128$.

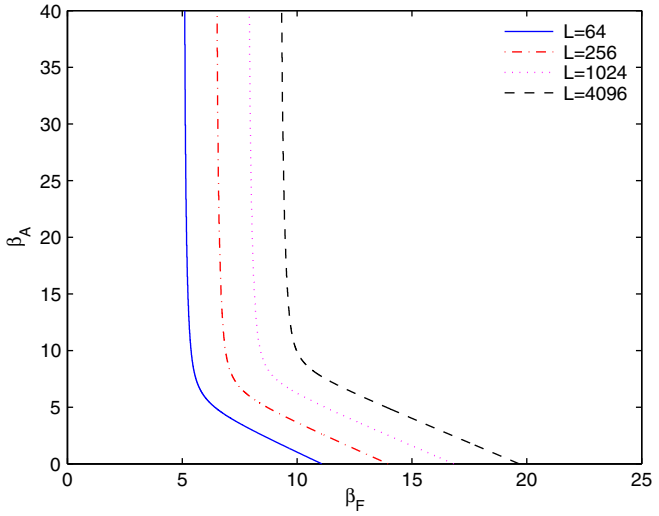

FIG. 7 (color online). Peak curves of the susceptibility χ_z in the $\beta_F - \beta_A$ plane for $L = 64$, 256, 1024, and 4096.

As for the scaling of the pseudocritical points with L, from Eqs. (15), we have that along lines parallel to the β_A axis $\langle z \rangle = 0$. Otherwise, we can fix a line $\beta_A = f(\beta_F)$ and solve

$$p(\beta_F, f(\beta_F)) = \frac{\log 2}{4L^2} \tag{20}$$

for β_F. In particular, from Eq. (16) and using the asymptotic expansion [70]

$$p(\beta_F, \beta_A \equiv 0) \sim \sqrt{\frac{2\beta_F}{\pi}} e^{-\beta_F} \left[1 + \mathcal{O}\left(\frac{1}{\beta_F}\right)\right], \tag{21}$$

we get for the two limiting cases $\beta_A \to 0, \infty$,

$$\beta_F^c(L)|_{\beta_A=0} \sim \log L^2 + \frac{1}{2}\log\log L^2 + \mathcal{O}(1) \tag{22}$$

$$\beta_F^c(L)|_{\beta_A=\infty} \sim \frac{1}{2}\log L^2 + \mathcal{O}(1); \tag{23}$$

shifting Eqs. (17) by Eqs. (22) and (23), $\langle z \rangle$ and $\langle \chi_z \rangle$ will fall on top of each other.

Inverting Eqs. (22) and (23), one can extract the critical behavior of the correlation length $\xi \sim L$ for $\beta_A \to 0, \infty$, where the prefactors come from the $\mathcal{O}(1)$ terms:

$$\xi|_{\beta_A=0} \sim \sqrt[4]{\frac{\pi \log^2 2}{2\beta_F}} \cdot e^{\frac{1}{2}\beta_F} \tag{24}$$

$$\xi|_{\beta_A=\infty} \sim \sqrt{\frac{\log 2}{4}} \cdot e^{\beta_F}. \tag{25}$$

Similar expressions will hold for any direction $\beta_A = f(\beta_F)$ along which the continuum limit $\beta_F \to \infty$ is taken.[18] At $T > 0$, one can simply substitute $L^2 \to L_s \cdot L_t$ in Eqs. (18), (19), (22), and (23). The scaling behavior remains thus, up to a factor, unchanged when taking the thermodynamic limit $L_s \to \infty$; the critical behavior will persist for any fixed L_t, i.e., at any temperature.

Compare now the above scaling with the critical behavior of the Kosterlitz-Thouless universality class [72–74] as a function of the reduced coupling β_{red}:

$$\xi_{KT} \sim K e^{A\beta_{\text{red}}^{\nu}} \tag{26}$$

$$\beta_{\text{red}}^{-1} = |\beta^{-1} - \beta_c^{-1}| \propto |T - T_c|. \tag{27}$$

Albeit with a different critical exponent, $\nu = 1$ and $\nu = 1/2$, respectively, both cases show essential scaling; i.e., the correlation length diverges exponentially as one approaches the critical coupling, which in our case is $\beta_F^c = \infty$. Mimicking now a well-known argument [73,74], we can give a simple explanation for the behavior found in Eqs. (24) and (25). At weak coupling, the free energy cost to change the sign of a plaquette is $f \sim 2\beta_F$; the density of negative plaquettes will thus be controlled by a Boltzmann factor $\rho \sim \exp(-f)$. On the other hand, the possible positions for this sign flip will scale like L^2, and the balance between free energy and entropy gives $L \sim \rho^{-1/2} = \exp(\beta_f) \simeq \xi$.[19] Up to the power correction for the $\beta_A = 0$ case, Eq. (24), this simple argument works quite well, contrary to the XY model, in which it cannot explain renormalization effects leading to the nontrivial critical exponent $\nu = 1/2$. Moreover, since the minimal distance among vortices can be reliably estimated with that along a plane intersecting them, such a picture should (roughly) hold in higher dimensions as well.

We could in principle explore the similarities with the Kosterlitz-Thouless transitions further. Although, as far as we know, for the XY model, no local order parameter is available, one can couple the theory to an external magnetic field h and study the analytical continuation of the partition function $Z(\beta, h)$ to the complex plane. (Hyper)scaling relations will then hold among the critical exponents of ξ, of the magnetic susceptibility $\chi_h \sim \xi^{2-\eta}\log^{-2r}\xi$, of the specific heat C_s, and of the edge of the Lee-Yang zeroes [72]. We will avoid such a thorough analysis in our case, for which a dedicated paper would be needed. Let us, however, just briefly comment on two points. First, from Eq. (13), we can explicitly calculate the reduced partition function and the specific heat in our usual limiting cases:

[18] Of course, this only holds as long as $f(\beta_F) \sim \beta_F$ for large β_F.

[19] We wish to thank P. de Forcrand for useful comments about this point.

$$Z \underset{\beta_A \to 0}{\propto} \frac{1}{\beta_F} I_1(\beta_F) \tag{28}$$

$$Z \underset{\beta_A \to \infty}{\propto} \frac{e^{\beta_A}}{\sqrt{\beta_A^3}} \cosh \beta_F \tag{29}$$

$$C_s \underset{\beta_A \to 0}{=} \frac{3}{2\beta_F^2} \tag{30}$$

$$C_s \underset{\beta_A \to \infty}{=} 1 - \tanh^2 \beta_F. \tag{31}$$

Inserting Eqs. (22) and (23) into Eqs. (30) and (31) and assuming that no other contribution besides the singular one exists [72], we see that the critical behavior for C_s should change (continuously?) from $\log^{-2} L$ to L^{-2}. Second, in our case, we have direct access to a nonlocal, topological order parameter, for which we can determine a critical exponent, $z \sim ML^{-\beta}$; from Eq. (19), we have $\beta = 0$. If we would like to study the extended partition function $Z(\beta_F, \beta_A, h)$, we could simply add a term $S_h = hz$ to the action. Although a direct calculation would go beyond the scope of this paper, it is obvious that for fixed L a sufficient condition to align the center flux z is realized if $\beta_F \to \infty$; the fundamental coupling plays the role of a "mock" $\mathbb{Z}_2$ magnetic field. Indeed, from Eqs. (28) and (29), the zeros of Z in the complex β_F plane all lie on the imaginary axis, in agreement with the Lee-Yang theorem [75].

Let us finally turn to the continuum limit. From the above discussion, it is clear that taking the thermodynamic limit $L \to \infty$ before the weak coupling limit $\beta_F \to \infty$, as one should, i.e., taking the Euclidean volume $V = (aL)^2 \to \infty$ [or, at finite temperature, $V_s = (aL_s) \to \infty$], the theory remains stuck in the disordered phase $\langle z \rangle = 0$: no vortex topological sector can be defined, and the superselection rule of Eq. (2) is not realized.

On the other hand, assuming that the scaling of the string tension σ with the lattice spacing a, known analytically for $\beta_A = 0$,

$$\beta_F = \frac{4}{a^2 g^2}$$
$$\sigma = \frac{3}{8} g^2, \tag{32}$$

will hold up to a different prefactor along any line $f(\beta_F) \propto \beta_F$, we get

$$V = (aL)^2 = \frac{3}{2} \frac{L^2}{\sigma \beta_F}. \tag{33}$$

Keeping now the volume V fixed as the continuum limit is approached, the values of the coupling at which one needs to simulate for fixed L will scale as $\beta_F \sim L^2$, i.e., much higher than the pseudocritical coupling $\beta_F^c \sim \log L$. The theory will thus be in a pseudo-ordered phase with $\langle z \rangle = 1$: on a *finite* Euclidean $d = 2$ torus, the Wilson action can admit well-defined $\mathbb{Z}_2$ topological sectors.[20]

B. $d = 3$

Increasing the dimensions to $d = 3$, we expect interactions to arise among parallel planes, since vortices are now extended, one-dimensional objects. The simple picture we have found in $d = 2$ will probably not work anymore, and less trivial critical exponents might arise. Still, fluxes are inherently two-dimensional objects, and most of the dynamics should thus take place on planes; many features of the $d = 2$ case should therefore survive. To check this, we have performed sets of Monte Carlo simulations along different lines in the $\beta_F - \beta_A$ plane. Results are reported for $\beta_A = 0$, $\beta_F = 0.5$, 0.75 and lattice sizes between $L = 24$ and $L = 80$; other parameters have been checked and give a consistent picture.

In the $\beta_A = 0$ case, approximately 20 to 50 simulations at coupling steps $\delta\beta_F$, each with 10^6 independent configurations, were performed for each volume L^3. The data have been reweighted [79,80] to determine the peak values $\beta_F^c(L)$ and $\chi_z(\beta_F^c(L))$; this was viable only up to $L \sim 64$. Indeed, as we shall see below, the $d = 3$ case shows a similar scaling behavior as Eq. (22), i.e., a logarithmic scaling of $\beta_F^c(L)$ to a critical coupling $\beta_F^c = \infty$. This has a practical drawback: the absolute width of the transition, i.e., the overall interval $\Delta\beta_F$ one needs to simulate, varies very slowly, while the step width $\delta\beta_F$ one must scan in order to keep the density of states computationally feasible decreases dramatically with L, and the computational cost becomes eventually unmanageable.

Results for all volumes considered are resummed in Table I, where the steps $\delta\beta_F$ are also listed, along with the value of the center flux and, for sake of completeness, of the specific heat at the pseudocritical point. To cross-check scaling results, similar simulation steps and statistics have also been used for the other volumes not included in the reweighting. The data can be well fit with the ansatz:

$$\chi_z(\beta_F^c(L)) \sim AL^{2-\eta} \log^{-2r} L (1 + \mathcal{O}(L^{-1})) \tag{34}$$

$$z(\beta_F^c(L)) \sim ML^{-\beta}(1 + \mathcal{O}(L^{-1})) \tag{35}$$

$$\beta_F^c(L) \sim C \log L^2 + D \log\log L^2 + \mathcal{O}(1). \tag{36}$$

For χ_z, we get $A = 0.21(1)$, $r = -0.134(10)$, $\eta = 0.0001(100)$, and $\chi^2/\text{d.o.f.} = 5.7$; constraining

[20] Some interpretation issues, of course, arise in this case. For example, speaking of zero temperature for a compactified, periodic time is at best misleading. Of course, one could also consider the case $L_s^2 \sim \beta_F$, but to fix the temperature independently, one must resort to an anisotropic (Hamiltonian) setup [76]. Transitions on finite toruses in the large N limit of the $d = 2$ Yang-Mills theories have been the subject of intense investigations; see Refs. [77,78] and references therein.

TABLE I. Position and height of the susceptibility peaks along β_F in $d = 3$. The third and fourth lines give the values of the order parameter and of the specific heat at the pseudocritical point $\beta_F^c(L)$; the last line gives the coupling steps for the simulations used in the reweighting.

	$L = 24$	$L = 32$	$L = 40$	$L = 48$	$L = 64$
$\beta_F^c(L)$	5.61(1)	5.930(5)	6.174(2)	6.383(5)	6.700(5)
$\chi_z(\beta_F^c(L))$	152.90(4)	282.83(8)	454.24(12)	666.6(2)	1217.4(3)
$z(\beta_F^c(L))$	0.392(3)	0.3610(15)	0.3364(13)	0.3213(16)	0.2908(16)
$C_s(\beta_F^c(L))$	0.1078(3)	0.0957(1)	0.0877(2)	0.0817(3)	0.0739(4)
$\delta\beta_F$	0.025	0.0125	0.00625	0.003125	0.0015625

$\eta = 0$ gives again $A = 0.21(1)$, $r = -0.134(10)$ with $\chi^2/\text{d.o.f.} = 2.8$. For β_F^c, we get $C = 0.61(3)$ and $D = -0.42(5)$ with $\chi^2/\text{d.o.f.} = 0.7$; on the other hand, constraining $D = 0$, we get $C = 0.56(3)$, $\chi^2/\text{d.o.f.} = 0.6$. Finally, for the order parameter, we get $M = 1.26(5)$ and $\beta = 0.35(1)$ with $\chi^2/\text{d.o.f.} = 1.4$. Overall, the biggest source of systematic error is given by the parametrization of the subleading corrections; leaving them out or parametrizing them differently leads to changes of up to 10% for some of the critical exponents, not included in our error estimates. Obviously, more data at higher volumes are needed to pin the numbers down.[21] The data for the susceptibility χ_z, rescaled by Eqs. (34) and (36), are plotted in Fig. 8, showing very good agreement also for the volumes that have not been included in the reweighting analysis. In Fig. 9, we show the scaling of the order parameter z according to Eqs. (35) and (36); the agreement for $L \gtrsim 40$ is again very good. As for the specific heat, a fit of the data in Table I with a logarithmic ansatz $C_s \sim \log^{-\alpha} L$ gives $\alpha = 1.4(1)$ with a $\chi^2/\text{d.o.f.} = 0.5$. The signal-to-noise ratio for the Monte Carlo is, however, not so good in this case, reflecting itself in the quality of the reweighted data; more statistics would be definitely needed, and, anyway, checking any (hyper)scaling relation is beyond our goals.

The above result is quite surprising. Indeed, in contrast to $d = 2$, one could have expected the $\mathbb{Z}_2$ monopole to control the open center vortices, since the density of the latter is proportional to that of the former. However, although monopoles per unit volume steadily decrease beyond the crossover, open vortices "connecting" them still cause a critical behavior cumulating to $g^2 \to 0$.[22] A possible explanation could be that their length increases more than linearly with the lattice size; multiple bendings in orthogonal directions would be enough to randomize the fluxes. A direct investigation of any geometrical properties of open vortices is, however, beyond the scope of this paper, since Eq. (9) is nonlocal and gauge invariant and does not allow us to isolate the topological defects on the planes.

Going now to the $\beta_A \neq 0$ case, since the $\mathbb{Z}_2$ monopoles undergo a crossover also in the low β_F region of the phase diagram of Fig. 2, one would expect the center flux to behave as in the β_F case: one should find along β_A a similar scaling as in Eqs. (34) and (36). Also, the transition lines should not be effected by the bulk transition associated with the unphysical $\mathbb{Z}_2$ gauge degrees of freedom. However, such a strong transition unavoidably makes any simulation near it quite noisy; on top of that, the biased Metropolis algorithm, with, e.g., three microcanonical steps, gets inefficient as β_F gets small and β_A gets large, reaching for z and χ_z, around the peaks of the latter, integrated autocorrelation times of the order 10^4–10^5 for $24 \leq L \leq 40$. Passable data were therefore only accessible for three volumes, while gathering enough statistics to reweight the susceptibility was out of the question. We have thus limited ourself to a consistency check near the bulk transition with a scaling ansatz similar to Eqs. (34)–(36):

$$\chi_z(\beta_A^c(L)) \sim AL^2 \log^{-2r} L + \mathcal{O}(L) \tag{37}$$

$$z(\beta_A^c(L)) \sim ML^{-\beta}(1 + \mathcal{O}(L^{-1})) \tag{38}$$

$$\beta_A^c(L) \sim C \log L^2 + \mathcal{O}(1); \tag{39}$$

no fit has been attempted. The scaling of the pseudocritical point and of the order parameter are consistent with the $d = 2$, $\beta_A = \infty$ case, $C = 1/2$ and $\beta = 0$, as can be seen from Fig. 10. On the other hand, the peaks of χ_z are quite noisy, and even a consistency check for the logarithmic exponent is hopeless. In Figs. 11 and 12, we show the results for the simulations along $\beta_F = 0.5$ and $\beta_F = 0.75$, lying, respectively, left and right of the bulk transition, rescaled by Eqs. (37) and (39) with a "guessed" value for $r = -1/2$; of course, further work would be needed to determine the critical exponents reliably.

[21] Another possible issue could be the nonergodicity of our setup in the ordered phase. Indeed, a "good" algorithm would need to change boundary conditions to enable tunneling among different topological sectors around the transition, just like a cluster algorithm in an Ising model allows tunneling among different orientations of the spins in the spontaneously magnetized phase. See, e.g., Ref. [23] for possible solutions to the problem. Implementing such algorithm is obviously beyond the scope of this paper.

[22] A somewhat cryptic comment regarding a possible critical behavior, going as far as taking the XY model as a paradigm, can be found in Ref. [37].

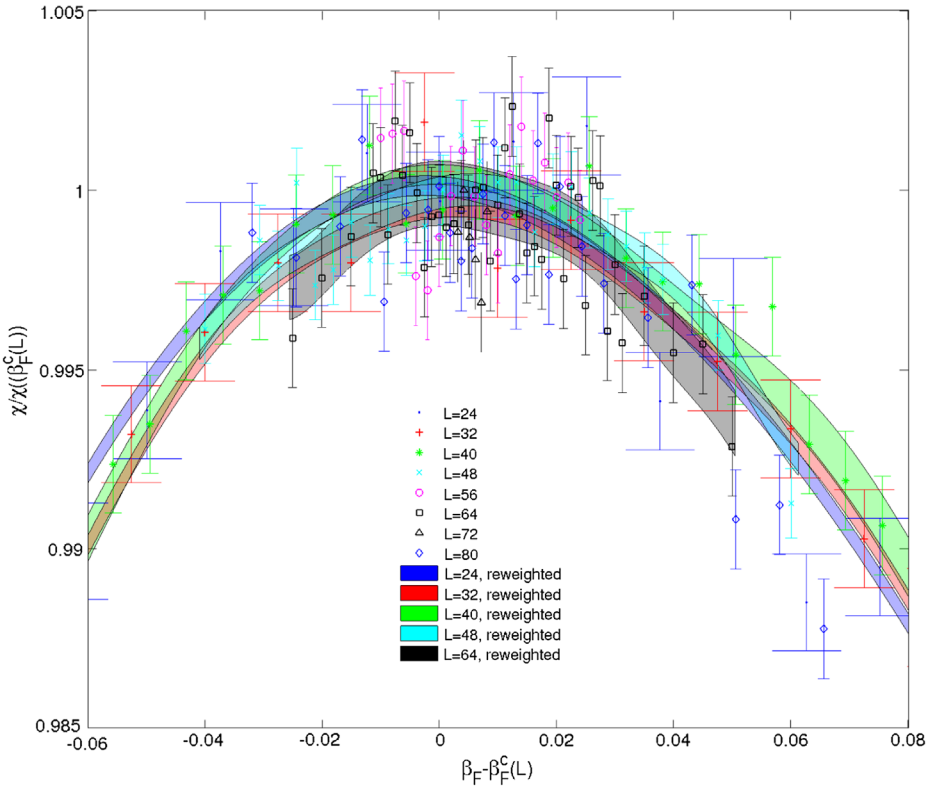

FIG. 8 (color online). Data for the susceptibility of the order parameter in $d = 3$, including the reweighted curves, rescaled with the FSS ansatz in Eqs. (34) and (36).

We have also checked via Monte Carlo simulations that all of the above results generalize to $T > 0$ by simply substituting $L^2 \to L_s \cdot L_t$ in all the scaling relations for temporal fluxes, while the behavior of all spacial fluxes remains unchanged. Again, as in the $d = 2$ case, this implies that, along any line in the $\beta_F - \beta_A$ plane, when taking the thermodynamic limit before the weak coupling limit, i.e., sending the volume to infinity, the $d = 3$ theory remains stuck in the disordered phase $\langle z \rangle = 0$; again, Eq. (2) is not realized.

What about the fixed volume limit? Taking as a blueprint for the continuum limit along any direction the scaling of the string tension along β_F [81],

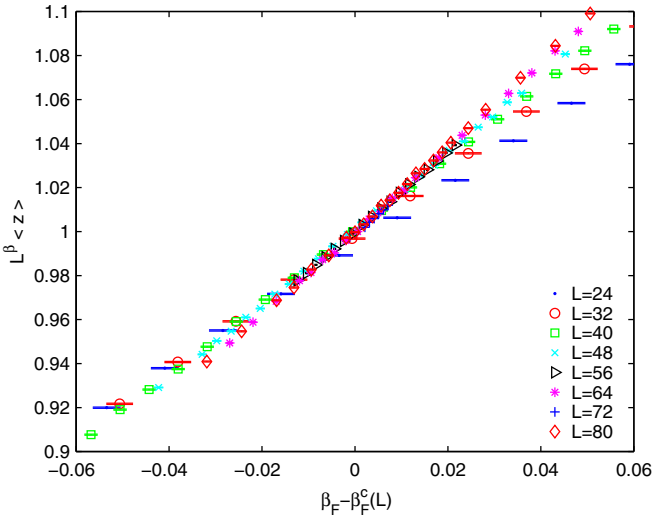

FIG. 9 (color online). FSS for the order parameter z as a function of the rescaled coupling as in Eq. (35).

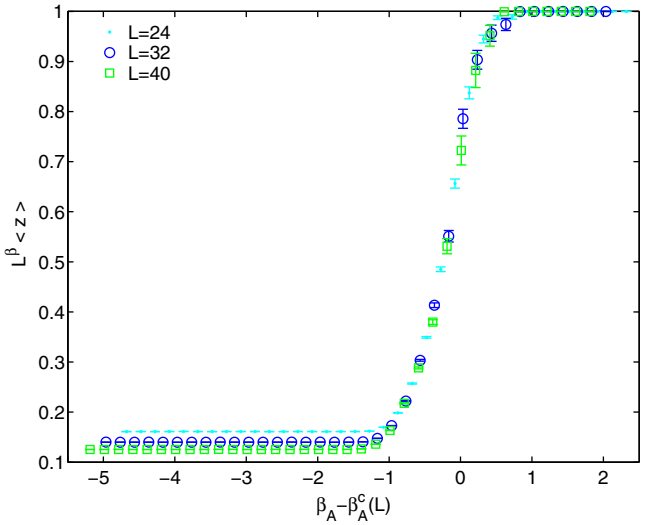

FIG. 10 (color online). FSS for the order parameter z along the $\beta_F = 0.5$ line with the ansatz in Eqs. (37) and (38).

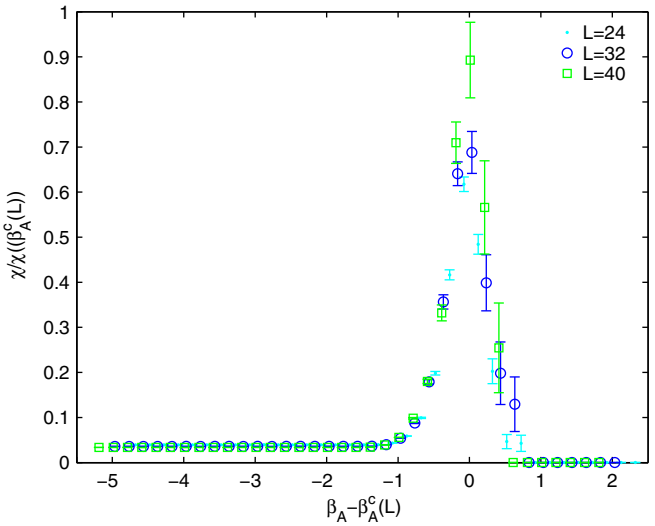

FIG. 11 (color online). FSS for the susceptibility χ_z along the $\beta_F = 0.5$ line with the ansatz in Eqs. (37) and (39).

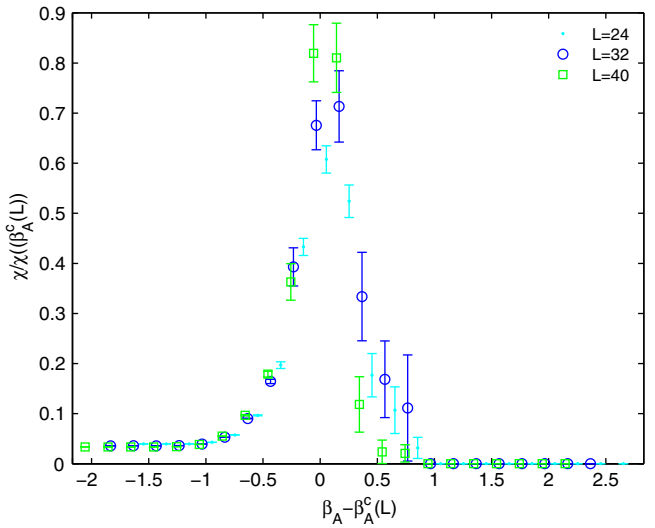

FIG. 12 (color online). FSS for the susceptibility χ_z along the $\beta_F = 0.75$ line with the ansatz in Eqs. (37) and (39).

$$\beta_F = \frac{4}{ag^2}$$
$$a\sqrt{\sigma} = \frac{c_0}{\beta_F} + \frac{c_1}{\beta_F^2} + \mathcal{O}\left(\frac{1}{\beta_F^3}\right), \tag{40}$$

we get immediately

$$V = (aL)^3 \propto \frac{L^3}{\beta_F^3\sqrt{\sigma^3}}. \tag{41}$$

Keeping again V fixed as the continuum limit is approached, the values of the coupling corresponding to a given L will now scale as $\beta_F \sim L$; again, as in $d = 2$, they will always be much higher than the pseudocritical coupling $\beta_F^C \sim \log L$, and the Wilson action could admit well-defined $\mathbb{Z}_2$ topological sectors on a finite $d = 3$ torus.

TABLE II. Position and height of the susceptibility peaks along β_F in $d = 4$.

	$L = 12$	$L = 16$	$L = 20$	$L = 24$
$\beta_F^c(L)$	3.15(5)	3.40(5)	3.60(5)	3.75(5)
$\chi_z(\beta_F^c(L))$	24(1)	42(1)	66(1)	95(1)

TABLE III. Position of the susceptibility peaks along β_A in $d = 4$ for $\beta_F = 1.0$, 1.2, and 1.3; the heights are all compatible with the results in Table II.

	$L = 16$	$L = 20$	$L = 24$
$\beta_F = 1.0$	1.845(25)	1.923(25)	1.987(25)
$\beta_F = 1.2$	1.695(25)	1.773(25)	1.837(25)
$\beta_F = 1.3$	1.62(1)	1.70(10)	1.76(1)

C. $d = 4$

The positions of the peaks of χ_z, as obtained in the simulations along the $\beta_A = 0$, $\beta_F = 1.0$, $\beta_F = 1.2$, and $\beta_F = 1.3$ lines, all within phase I of Fig. 3, are shown in Tables II and III. We have again limited ourselves to a consistency check with a scaling ansatz of the form

$$\chi_z(\beta_F^c(L)) \sim AL^2 + \mathcal{O}(L) \tag{42}$$

$$z(\beta_F^c(L)) \sim ML^{-\beta}(1 + \mathcal{O}(L^{-1})) \tag{43}$$

$$\beta_F^c(L) \sim C\log L^2 + \mathcal{O}(1). \tag{44}$$

Results are shown in Figs. 13 and 14 for the order parameter and its susceptibility along the β_F axis; up to the values of C, the behavior along the lines parallel to the β_A axis is basically the same (see, e.g., Fig. 15). From the data in Table II, we can estimate $C = 0.46(3)$, compatible with $1/2$, while for those in Table III, we get $C = 0.18(3)$; in all cases, β is compatible with 0.

Direct simulations at $T > 0$ give again the same scaling with $L^2 \to L_s \cdot L_t$ for the temporal fluxes, while spacial fluxes remain unchanged. As in the $d = 2$ and $d = 3$ cases, in the thermodynamic limit, the theory remains therefore stuck in the disordered phase. Moreover, starting from the two-loop beta function, the running of the physical scale with $\alpha_{\text{lat}} = g^2/(4\pi)$ is given by

$$\log(a^2\sigma) = -\frac{4\pi}{\beta_0}\alpha_{\text{lat}}^{-1} + \frac{2\beta_1}{\beta_0^2}\log\left(\frac{4\pi}{\beta_0}\alpha_{\text{lat}}^{-1}\right) + c + \mathcal{O}(\alpha_{\text{lat}}), \tag{45}$$

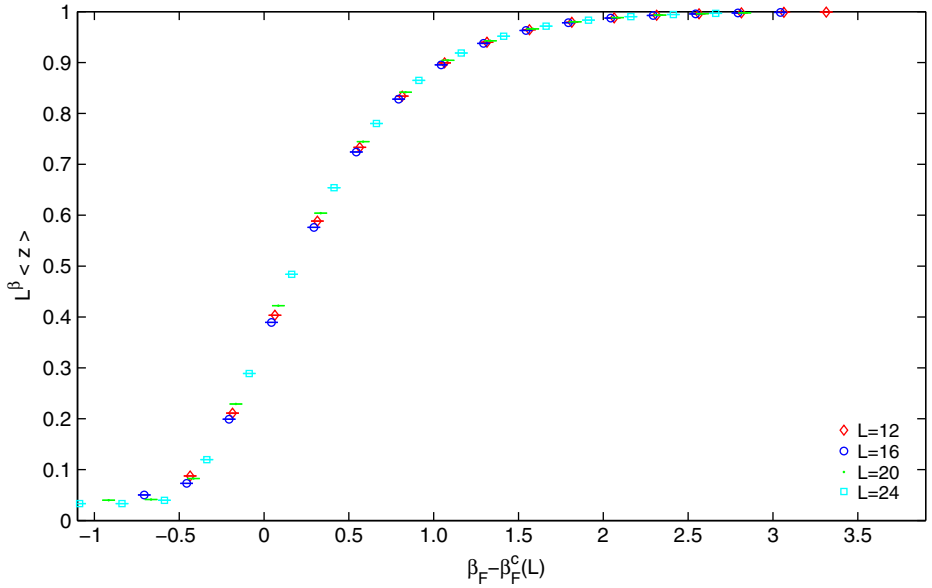

FIG. 13 (color online). FSS as in Eqs. (43) and (44) for z in $d = 4$ along the β_F axis.

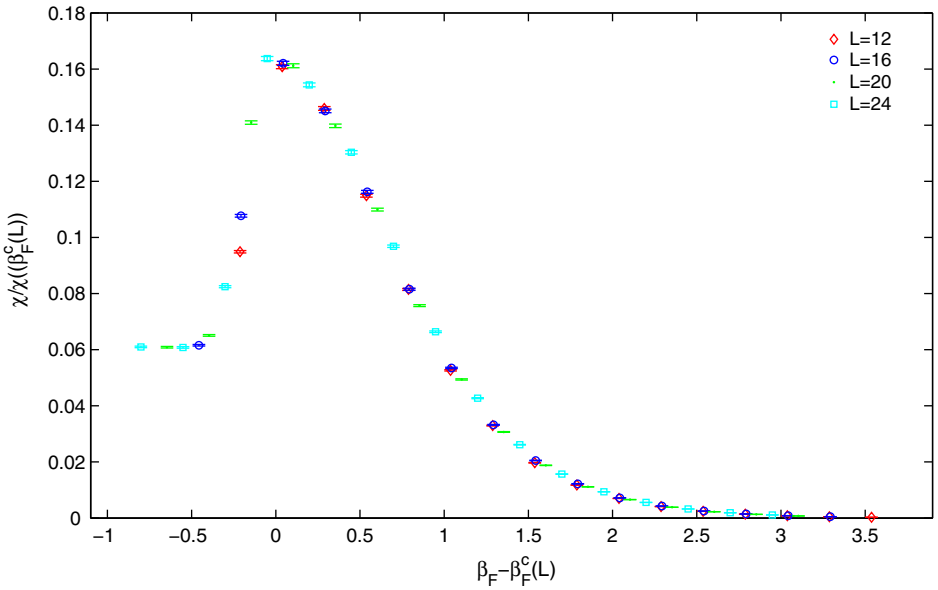

FIG. 14 (color online). FSS as in Eqs. (42) and (44) for χ_z in $d = 4$ along the β_F axis.

where $c = \log \frac{\sigma}{\Lambda_{\rm lat}^2}$ and $\beta_0 = \frac{22}{3}$, $\beta_1 = \frac{68}{3}$, i.e., from Eq. (7):

$$V = (aL)^4 \propto L^4 \left(\frac{4\pi^2}{\beta_0}\beta_F\right)^{\frac{4\beta_1}{\beta_0^2}} e^{-\frac{8\pi^2}{\beta_0}\beta_F}. \tag{46}$$

When trying to keep the volume V fixed as $\beta_F \to 0$, up to log log corrections, the coupling should scale as

$$\beta_F \sim \frac{\beta_0}{4\pi^2} \log L^2; \tag{47}$$

the coefficient C in Eq. (44) is, however, larger than that coming from the beta function, and the simulation parameters will lie in the disordered phase. Topological sectors will always be ill defined also on a finite torus T^4. The same holds along the lines parallel to the β_A axis (see Table III); in this case, from Eq. (7), the coefficient in Eq. (47) coming from the beta function Eq. (45) is $3\beta_0/(32\pi^2)$, again smaller than the corresponding value of C.

As discussed in Sec. II B, we have excluded phase II (see Fig. 3) from the simulations. As mentioned above, vortex topology is, however, well understood in this case: the

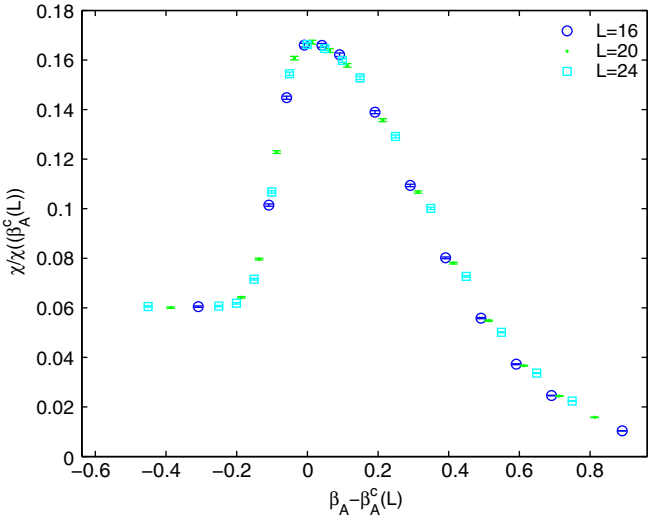

FIG. 15 (color online). FSS as in Eqs. (42) and (44) for χ_z in $d = 4$ along the $\beta_F = 1.3$ axis.

results of Refs. [21,22,29,47,60] show that, in contrast to phase I in $d = 4$ and to the $d = 2$ and 3 cases, the theory possesses well-defined $\mathbb{Z}_2$ topological sectors in the continuum limit.

IV. CONCLUSIONS

We have studied a topological order parameter, the center flux z defined in Eqs. (10) and (11), for the $SU(2)$ mixed action in $2 \le d \le 4$. Its ordered phase, $\langle z \rangle = 1$, corresponds to well-defined $\pi_1(SO(3)) = \mathbb{Z}_2$ topological sectors, i.e., to a vacuum satisfying the superselection rule of Eqs. (2) and (4), while for $\langle z \rangle = 0$, the vacuum state is disordered, and no center topology can be defined. This reminds us of a quantum phase transition; however, one does not switch between vacua by tuning a physical parameter. Rather, the choice of dimensions and the symmetry of the discretized action control in which phase the theory will be in the continuum limit.

More specifically, discretized actions transforming in the fundamental representation possess a disordered vacuum, with z showing an essential scaling to the critical coupling $\beta_c = \infty$. The critical exponent for the correlation length ξ is $\nu = 1$, i.e., $\beta_c(\xi) \propto \log \xi$; explicit log log ξ corrections to scaling can be shown to exist for some choice of parameters. The susceptibility of the center flux scales as $\chi_z(\xi) \propto \xi^2$ in $d = 2$ and $d = 4$, while the order parameter itself scales trivially in these cases. On the other hand, in $d = 3$, at least along the β_F axis, the center flux has a nontrivial critical exponent, $z(\xi) \propto \xi^{-\beta}$, with $\beta = 0.35(1)$, while a logarithmic correction can be explicitly determined for the scaling of its susceptibility, $\chi_z(\xi) \sim \xi^2 \log^{-2r} \xi$, with $r = -0.134(10)$; similar corrections might also be present along other lines in the $\beta_F - \beta_A$ diagram, but more statistics would be needed to reach a conclusive result. A tentative critical exponent for the specific heat, $C_s(\xi) \sim \log^{-\alpha} \xi$, gives $\alpha = 1.4(1)$, but with still high systematic errors. We have made no attempt to investigate any (hyper)scaling relations among such exponents; this would probably require a full analysis of the Lee-Yang zeros [72]. Such behavior persists in all dimensions at $T > 0$.

Vice versa, the topological classification of Eq. (1) and thus the superselection rule of Eqs. (2) and (4) can be realized by the vacuum state of lattice actions transforming in the adjoint representation; phase II in $d = 4$ (see Fig. 3) is such an example [21,22,29]. Large-scale simulations with the adjoint action are hampered by strong finite-volume effects [27,28,38]. Therefore, although the techniques used in Refs. [21,22,29] to tame them could also work in $d = 3$, a more viable alternative, applicable also in $d = 2$, would be to resort to positive plaquette models [14,55,56], where topological sectors are always well defined since the operator given in Eq. (9) takes "by construction" the values dictated by the assigned boundary conditions. Indeed, a one-to-one mapping between configurations in such a lattice discretization and those of the adjoint Wilson action with well-defined vortex sectors was conjectured in Ref. [27] and explicitly constructed in Ref. [29]. Finally, an ordered vacuum could also be realized for a finite torus in $d = 2, 3$; here, one could exploit the power-law scaling of the physical mass with the coupling to define topological sectors when $L \to \infty$ and $a \to 0$ with the volume $V = (aL)^d$ kept fixed.

The above findings do not contradict universality, since nonperturbatively the equivalence between fundamental and adjoint actions can only hold as long as no lattice artifacts are present [27–29,36–39], while as we have seen for some discretizations, the density of $\mathbb{Z}_2$ monopoles cannot vanish at any finite coupling [37]. Does, however, such a result have any physical consequences? The vacua of the two different phases can be essentially characterized by the type of $\mathbb{Z}_2$ vortices they can carry:

(i) The ordered phase allows topological center vortices "*à la* 't Hooft" [12,13]. A confinement mechanism based on the superselection rule of Eqs. (2) and (4) can be realized; at finite temperature, the change in the vortex free energy as measured via Eq. (3) is thus a valid test to establish how the symmetry is broken in the transition to the deconfined phase [21,22,29]. No fundamental fields are allowed in this case [12,13,31]; however, adjoint fermions can be easily incorporated in such a scenario. It might therefore be interesting to investigate the vacuum properties of the $SU(2)$ gauge theory coupled to adjoint fermions, a popular candidate for infrared conformality [65]. Numerical tests with the adjoint Wilson action or positive plaquette model should be viable.

(ii) The disordered phase is dominated by (one huge, percolating?) open vortices, reminding us of the

Nielsen-Olesen "spaghetti vacuum" [4]. Such open vortices are not topological according to Eq. (1); Eqs. (2) and (4) cannot be applied. One might conjecture some relationship with P vortices [2,15,16], although it is still unclear how to test such a hypothesis, since the center flux z is gauge invariant and constructed out of pure $SO(3)$ variables while P vortices are gauge dependent and built out of the $\mathbb{Z}_2$ gauge degrees of freedom. Moreover, such open vortices persist at any temperature, not disappearing above T_C. This disordered vacuum is detached from the boundary conditions chosen and is therefore compatible with the presence of fundamental matter fields. Of course, Eq. (3) is ill defined in this case; whether any vortex related order parameter for the confinement-deconfinement phase transition could be defined remains an open question.

ACKNOWLEDGMENTS

We are indebted to F. Bursa for precious correspondence on the $d = 2$ Yang-Mills theory. We want to thank B. Lucini, P. de Forcrand, and D. Campagnari for critical reading of the manuscript; we also wish to thank R. Kenna for interesting discussions on Lee-Yang and Fisher zeroes. A special thanks goes to E. Rinaldi for correspondence on the implementation of the biased Metropolis algorithm. This work was supported by the Bundesministerium für Bildung und Forschung under Contract No. BMBF-05P12VTFTF.

[1] A. M. Jaffe and E. Witten, Clay Mathematics Institute Millenium Prize problem (2000), http://www.claymath.org/millennium/Yang-Mills_Theory/yangmills.pdf.
[2] J. Greensite, *An Introduction to the Confinement Problem*, Vol. 821 (Springer-Verlag, Berlin, Heidelberg, 2011), p. 1.
[3] T. Wu and C.-N. Yang, *Properties Of Matter Under Unusual Conditions*, edited by H. Mark and S. Fernbach (Interscience, New York, 1969).
[4] H. B. Nielsen and P. Olesen, Nucl. Phys. **B61**, 45 (1973).
[5] G. 't Hooft, Nucl. Phys. **B79**, 276 (1974).
[6] S. Mandelstam, Phys. Lett. **53B**, 476 (1975).
[7] A. M. Polyakov, Nucl. Phys. **B120**, 429 (1977).
[8] P. Goddard, J. Nuyts, and D. I. Olive, Nucl. Phys. **B125**, 1 (1977).
[9] S. Mandelstam, Phys. Rev. D **19**, 2391 (1979).
[10] E. J. Weinberg, Nucl. Phys. **B167**, 500 (1980).
[11] N. Seiberg and E. Witten, Nucl. Phys. **B426**, 19 (1994).
[12] G. 't Hooft, Nucl. Phys. **B138**, 1 (1978).
[13] G. 't Hooft, Nucl. Phys. **B153**, 141 (1979).
[14] G. Mack and E. Pietarinen, Nucl. Phys. **B205**, 141 (1982).
[15] L. Del Debbio, M. Faber, J. Greensite, and S. Olejnik, Phys. Rev. D **55**, 2298 (1997).
[16] K. Langfeld, H. Reinhardt, and O. Tennert, Phys. Lett. B **419**, 317 (1998).
[17] T. G. Kovacs and E. Tomboulis, Phys. Rev. Lett. **85**, 704 (2000).
[18] A. Hart, B. Lucini, Z. Schram, and M. Teper, J. High Energy Phys. 06 (2000) 040.
[19] P. de Forcrand, M. D'Elia, and M. Pepe, Phys. Rev. Lett. **86**, 1438 (2001).
[20] P. de Forcrand and L. von Smekal, Phys. Rev. D **66**, 011504 (2002).
[21] G. Burgio, M. Fuhrmann, W. Kerler, and M. Muller-Preussker, Phys. Rev. D **74**, 071502 (2006).
[22] G. Burgio, M. Fuhrmann, W. Kerler, and M. Muller-Preussker, Phys. Rev. D **75**, 014504 (2007).
[23] L. von Smekal, Nucl. Phys. B, Proc. Suppl. **228**, 179 (2012).
[24] A. Gonzalez-Arroyo, arXiv:hep-th/9807108.
[25] G. Burgio, R. De Pietri, H. A. Morales-Tecotl, L. F. Urrutia, and J. D. Vergara, Nucl. Phys. **B566**, 547 (2000).
[26] H. Reinhardt, Phys. Lett. B **557**, 317 (2003).
[27] P. de Forcrand and O. Jahn, Nucl. Phys. **B651**, 125 (2003).
[28] I. Halliday and A. Schwimmer, Phys. Lett. **102B**, 337 (1981).
[29] A. Barresi and G. Burgio, Eur. Phys. J. C **49**, 973 (2007).
[30] B. Svetitsky and L. G. Yaffe, Nucl. Phys. **B210**, 423 (1982).
[31] T. D. Cohen, Phys. Rev. D **90**, 047703 (2014).
[32] A. Gonzalez-Arroyo and M. Okawa, Phys. Rev. D **27**, 2397 (1983).
[33] M. G. Perez, A. Gonzalez-Arroyo, and M. Okawa, Int. J. Mod. Phys. A **29**, 1445001 (2014).
[34] C. Sachrajda and G. Villadoro, Phys. Lett. B **609**, 73 (2005).
[35] E. Lubkin, Ann. Phys. (Berlin) **23**, 233 (1963).
[36] G. Mack and V. Petkova, Ann. Phys. (Berlin) **123**, 442 (1979).
[37] G. Mack and V. Petkova, Z. Phys. C **12**, 177 (1982).
[38] I. Halliday and A. Schwimmer, Phys. Lett. **101B**, 327 (1981).
[39] S. R. Coleman, *Gauge Theories In High Energy Physics, Part 1, Proceedings of the Les Houches Summer School, Session XX* (Cambridge, Massachusetts, 1982), p. 461.
[40] G. Burgio, *Proc. Sci.*, LATTICE2007 (2007) 292.
[41] G. Burgio, *Proc. Sci.*, LATTICE2013 (2014) 493.
[42] M. Creutz and K. Moriarty, Phys. Rev. D **25**, 1724 (1982).
[43] M. Creutz and K. Moriarty, Nucl. Phys. **B210**, 50 (1982).
[44] J. Drouffe, K. Moriarty, and G. Munster, Phys. Lett. **115B**, 301 (1982).
[45] R. Ardill, K. Moriarty, and M. Creutz, Comput. Phys. Commun. **29**, 97 (1983).
[46] R. Ardill, M. Creutz, and K. Moriarty, J. Phys. G **10**, 867 (1984).
[47] A. Barresi, G. Burgio, and M. Muller-Preussker, Phys. Rev. D **69**, 094503 (2004).

[48] J. Drouffe and J. Zuber, Nucl. Phys. **B180**, 264 (1981).
[49] J. Greensite and B. Lautrup, Phys. Rev. Lett. **47**, 9 (1981).
[50] G. Bhanot and M. Creutz, Phys. Rev. D **24**, 3212 (1981).
[51] M. Baig and A. Cuervo, Nucl. Phys. **B280**, 97 (1987).
[52] M. Baig and A. Cuervo, Phys. Lett. B **189**, 169 (1987).
[53] M. Baig and A. Cuervo, Nucl. Phys. B, Proc. Suppl. **4**, 21 (1988).
[54] F. Bursa and M. Teper, Phys. Rev. D **74**, 125010 (2006).
[55] V. Bornyakov, M. Creutz, and V. Mitrjushkin, Phys. Rev. D **44**, 3918 (1991).
[56] J. Fingberg, U. M. Heller, and V. Mitrjushkin, Nucl. Phys. **B435**, 311 (1995).
[57] A. Barresi, G. Burgio, and M. Muller-Preussker, Nucl. Phys. B, Proc. Suppl. **106–107**, 495 (2002).
[58] A. Barresi, G. Burgio, and M. Muller-Preussker, Nucl. Phys. B, Proc. Suppl. **119**, 571 (2003).
[59] A. Barresi, G. Burgio, and M. Muller-Preussker, *Confinement 2003* (World Scientific, Singapore, 2003), p. 82.
[60] A. Barresi, G. Burgio, M. D'Elia, and M. Muller-Preussker, Phys. Lett. B **599**, 278 (2004).
[61] A. Barresi, G. Burgio, and M. Muller-Preussker, Nucl. Phys. B, Proc. Suppl. **129–130**, 695 (2004).
[62] G. Burgio, M. Fuhrmann, W. Kerler, and M. Muller-Preussker, *Proc. Sci*, LATTICE2005 (2006) 288.
[63] A. Bazavov and B. A. Berg, Phys. Rev. D **71**, 114506 (2005).
[64] A. Bazavov, B. A. Berg, and U. M. Heller, Phys. Rev. D **72**, 117501 (2005).
[65] B. Lucini, A. Patella, A. Rago, and E. Rinaldi, J. High Energy Phys. 11 (2013) 106.
[66] M. Hasenbusch and S. Necco, J. High Energy Phys. 08 (2004) 005.
[67] M. E. Fisher and M. N. Barber, Phys. Rev. Lett. **28**, 1516 (1972).
[68] K. Eriksson, N. Svartholm, and B. Skagerstam, J. Math. Phys. (N.Y.) **22**, 2276 (1981).
[69] C. Lang, P. Salomonson, and B. Skagerstam, Phys. Lett. **100B**, 29 (1981).
[70] M. Abramowitz and I. A. Stegun, *Handbook of Mathematical Functions with Formulas, Graphs, and Mathematical Tables* (Dover, New York, 1964).
[71] F. Bursa (private communication).
[72] R. Kenna and A. Irving, Nucl. Phys. **B485**, 583 (1997).
[73] J. Kosterlitz and D. Thouless, J. Phys. C **6**, 1181 (1973).
[74] J. Kosterlitz, J. Phys. C **7**, 1046 (1974).
[75] T. Lee and C.-N. Yang, Phys. Rev. **87**, 410 (1952).
[76] G. Burgio, A. Feo, M. J. Peardon, and S. M. Ryan (TrinLat), Phys. Rev. D **67**, 114502 (2003).
[77] R. Narayanan and H. Neuberger, J. High Energy Phys. 12 (2007) 066.
[78] A. Hietanen and R. Narayanan, Phys. Rev. D **86**, 085002 (2012).
[79] A. Ferrenberg and R. Swendsen, Phys. Rev. Lett. **61**, 2635 (1988).
[80] A. M. Ferrenberg and R. H. Swendsen, Phys. Rev. Lett. **63**, 1195 (1989).
[81] M. J. Teper, Phys. Rev. D **59**, 014512 (1998).